Int. J. Electrochem. Sci., 15 **(2020)** 458 – 469, doi: 10.20964/2020.01.73

International Journal of ELECTROCHEMICAL SCIENCE
www.electrochemsci.org

Effects on Structure and Electrochemical Performance of $Li[Li_{0.2}Ni_{0.15}Mn_{0.55}Co_{0.1}]O_2$ by Surface Modification with MnO_2

Zhang Hai-Lang [1,], Tian Jian-Kun [2], Wan Fu-Cheng[2], Tang Ting[1]*

[1] School of Chemical and Material Engineering, Jiangnan University,Wuxi 214122, Jiangsu Province, China
[2] Xinyang Vacational & Technical College , Xinyang 464000, Henan Province,China
[*]E-mail:.zhl8868@vip.163.com

Received: 3 September 2019 / *Accepted:* 2 November 2019 / *Published:* 30 November 2019

Lithium-rich $Li[Li_{0.2}Ni_{0.15}Mn_{0.55}Co_{0.1}]O_2$ cathode materials prepared by a sol-gel method were coated by various content of MnO_2(1%, 3%, 5% in mass) via high temperature sintering. The effects of surface modification with MnO_2 on crystal structure and morphology have been characterized by X-ray diffraction (XRD) and scanning electron microscope(SEM), which reveals that the bulk structures of all samples maintain a typical α-$NaFeO_2$ layered oxide structure and the surface becomes relatively rough after modification. Electrochemical performances were investigated by charge/discharge cycling tests performed at room temperature and 55 ºC, respectively. The 3wt.% MnO_2-coated material delivers discharge capacity of 253.8 $mAh{\cdot}g^{-1}$ and 312.2 $mAh{\cdot}g^{-1}$ with first columbic efficiency of 82% and 91% at room temperature and 55ºC, respectively, which are much higher than those of the pristine material, 236.7$mAh{\cdot}g^{-1}$with first columbic efficiency of 69% at 25 ºC and 298.2 $mAh{\cdot}g^{-1}$ with first columbic efficiency of 83% at 55 ºC. After 50 cycles, the 3wt.% coated material exhibits a capacity retention of 94%, compared to a capacity retention of 83% for the pristine one. The cyclic voltammetry measurement confirms that the MnO_2 modification facilitates the structural stability of the materials. The suppression of side reaction between active materials and electrolyte and the changes of the structure of MnO_2 coating layer during cycling, as well as more oxygen vacancies retention caused by MnO_2 would be responsible for the improvement of the electrochemical properties.

Keywords: lithium-ion battery; lithium-rich layered cathode; coating; MnO_2; electrochemical performance

1. INTRODUCTION

Since the first generation of the commercialization of $LiCoO_2$ proposed by Sony in 1990, the development of lithium-ion batteries has received great attention from researchers due to the high-capacity, energy density and environmental characteristics. However, compared with $LiCoO_2$, spinel and olivine families, in the last decade, a family of the lithium-rich layered oxides usually denoted as

$xLi_2MnO_3\cdot(1-x)LiMO_2$(0＜x＜1, M=Ni, Mn, Co, ect) have been widely investigated as a promising cathode material candidate because of their exceptional high capacity(about 200-300 $mAh\cdot g^{-1}$), low cost and improved safety[1-5]. Wang et al.[6] found that $Li[Li_{0.2}Ni_{0.13}Mn_{0.54}Co_{0.13}]O_2$ prepared by sol-gel method delivers a initial discharge capacity of 260.0 $mAh\cdot g^{-1}$(20 $mA\cdot g^{-1}$). According to the traditional de-intercalation mechanism of the layered materials which only considers the redox of the transition metal ions, the specific capacity of the lithium-rich cathode $Li[Li_{0.13}Mn_{0.57}Ni_{0.3}]O_2$ is only184 $mAh\cdot g^{-1}$. In practice, however, the first charge and discharge capacity can reach as high as 352 $mAh\cdot g^{-1}$ and 287 $mAh\cdot g^{-1}$, respectively[7]. This phenomenon indicates that lithium-rich materials own a special charge and discharge mechanism. If the upper voltage limit was controlled above 4.5V, the Ni^{2+} of the transition metal layer was oxidized to Ni^{4+} accompanied by the removal of Li^+ and there would be a process of electrochemical activation of the manganese ions which would be responsible for the high specific capacity for the Li-rich materials when the voltage charged to 4.8 V[8,9]. Despite this class of materials are considered to have special advantages in the field of electric vehicles(EV), the materials also have several disadvantages, such as large initial irreversible capacity loss, poor rate capability and low capacity retention, which greatly inhibit their practical application in the future[3,4].

A lot of efforts have been devoted to overcome the disadvantages of the lithium-rich materials. One of them consists in the cationic(Al, Mg, Fe et al.) and anionic(F, S , Cl et al.) substitution of the partial transition metal ions(Mn, Co, Ni) and oxygen ions, respectively, which is evidently efficient at the increase of capacity, whereas this method would sacrifice a cycle life and even result in safety issues[10,11]. Another route is surface modification which has been explored to be an effective approach to improve the electrochemical properties of the cathode materials. After years of continuous research, many progresses have been obtained in surface modification in term of the prevention of the side reaction between active materials and electrolyte, the suppression of the loss of oxygen and the improvement of conductivity of materials [12]. In the past years, many coating agent compounds, involving metal oxides(such as Al_2O_3[13], TiO_2[14], MgO[15], V_2O_5[16] and CeO_2[17]), phosphates(such as $FePO_4$[18], $AlPO_4$[19]), carbon[20] and fluorides(such as AlF_3[21,22) have been used to enhance the electrochemical properties of lithium-rich layered oxide cathodes. As reported[23,24], the MnO_2 has a voltage platform under 3.0 V which would be attributed to the reaction with Li^+ escaped from the lattice surface of the active materials. In this paper, the influences of the surface modification by MnO_2 on the structure and electrochemical performance of $Li[Li_{0.2}Ni_{0.15}Mn_{0.55}Co_{0.1}]O_2$ at room temperature and elevated temperature have been studied in detail.

2. EXPERIMENTAL SECTION

2.1. Synthesis of materials

$Li[Li_{0.2}Ni_{0.15}Mn_{0.55}Co_{0.1}]O_2$ powders were synthesized by sol-gel method with citric acid as a chelating agent. At first, the required amount of hydrated metal nitrate salts, lithium nitrate ($LiNO_3$, A.R.),nickel nitrate ($Ni(NO_3)_2\cdot4H_2O$, A.R.), manganese acetate ($Mn(AC)_2\cdot4H_2O$, A.R.) and cobalt nitrate ($Co(NO_3)_2\cdot4H_2O$, A.R.) were dissolved in deionized water to gain an aqueous solution. A 5wt.%

excess of $LiNO_3$ was used to compensate the volatilization loss of lithium element caused by high temperature. Then the prepared citric acid solution was added into the prepared solution with a molar ratio of metal ions : chelating agent = 1:1. The pH of the mixed solution was adjusted to 7~8 by adding ammonium hydroxide drop by drop with stirring constantly. In order to obtain a transparent xerogel, the mixed solution was evaporated at 80 ^oC for 6 h with vigorous stirring followed by drying at 120 ^oC for 12 h. And then the resulting gel was first pre-calcined at 500 ^oC for 6 h in air to ensure the complete decomposition of organic content. Finally, the target compounds were gained by calcining at 900 ^oC for 12 h in air.

For MnO_2-coated $Li[Li_{0.2}Ni_{0.15}Mn_{0.55}Co_{0.1}]O_2$ powders, the coated contents were controlled in 1wt.%, 3wt.%, and 5wt.%, respectively, using nanoscale MnO_2 as coating materials. $Li[Li_{0.2}Ni_{0.15}Mn_{0.55}Co_{0.1}]O_2$ powders were homogeneously dispersed into absolute ethyl alcohol solvent followed by a required amount of nanoscale MnO_2 added into the solution with continuous mechanically stirring at 40 ^oC until the alcohol completely volatilized. And then the obtained slurry was dried at 80 ^oC for 12 h in blast drying oven to remove the remaining alcohol followed by calcining at 450 ^oC for 6 h in air to gain the resultant MnO_2-coated $Li[Li_{0.2}Ni_{0.15}Mn_{0.55}Co_{0.1}]O_2$ powders.

2.2. Characterization of materials

All samples were characterized by X-ray diffraction (XRD,Bruker D8) with Cu Kα radiation between 10° and 90° in 2θ with a step size of 0.02° and scanning electron microscope (SEM, S4800) to identify the crystal structure and morphology of the materials. The element type and distribution in micro area were determined by Energy Dispersive X-ray Spectroscopy (EDS, Noran System Six).

2.3. Electrochemical measurement

Electrochemical performances were examined by assembling half-cells in CR2032 type coin cells. One coin cell is composed of cathode, lithium metal anode, Celgard 2325 porous polypropylene film as the separator and electrolyte consisting of 1 M LiPF6/EC + DEC (1:1, v/v). Active materials, acetylene black and polyvinylidene tetrafluoroethylene (PVDF) used as a binder were mixed in a mass ratio of 80:12:8, and fully ground in N-methyl-2-pyrrodidene (NMP) solvent. The resultant slurry was pressed onto Al foil with Doctor-blade technique followed by drying at 80 ^oC for12 h in a vacuum oven to obtain the cathode electrodes. The experimental cells were assembled in an argon-filled dry glove box (Mikrouna SUPER 1220/750, made in Shanghai) and the charge/discharge tests were carried out on a charge and discharge tester (Land CT2001,Wuhan in China) at room temperature and 55^oC, respectively, in the potential range of 2.0~4.8 V under different current densities.

The cyclic voltammetry (CV) can detect the polarization of electrodes and the red-ox reaction reversibility of the electrochemically active metal ions by examining the peak position, shape and size, as well as the potential changes with the changes in current. In this paper, the CV was tested on the IM6E type electrochemical workstation (ZAHENR， made in Germany) with a voltage range of 2~4.8 V at a scan rate of 0.01mV/s at room temperature.

3. RESULTS AND DISCUSSION

Fig.1 displays the XRD patterns of the bare and MnO_2-coated cathode materials. As showed, the clear and well defined diffraction peaks can be indexed as an α-$NaFeO_2$ layered structure with R-3m symmetry, except for several weak peaks around 20~25°, which are derived from superlattice structure attributed to the ordering of Li and Mn atoms in the transition-metal layer of a rock salt structure of Li_2MnO_3 with C2/m symmetry [25,26]. This suggests that the bulk structure does not change after surface modification with a little amount of MnO_2. By comparing the pristine with MnO_2-coated samples, no additional diffraction peaks belonging to MnO_2 could be detected, revealing that there could be a thin amorphous MnO_2 coating layer which only presents in the surface of the materials rather than diffuses into the bulk structure.

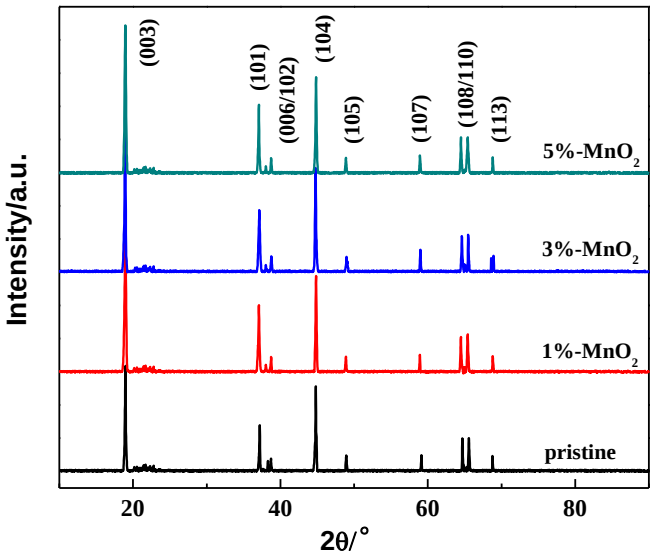

Figure 1. The XRD patterns of $Li[Li_{0.2}Mn_{0.55}Ni_{0.15}Co_{0.1}]O_2$ before and after MnO_2 surface modification.

Fig.2 shows the scanning electron images of the lithium-rich layered cathode $Li[Li_{0.2}Ni_{0.15}Mn_{0.55}Co_{0.1}]O_2$ before and after surface modification with MnO_2. As shown in the images, the surfaces of the samples coated with different amounts of MnO_2 become a little rough than that of the bare one whose surface is relatively smooth, which demonstrates that the MnO_2 oxides have successfully coated on the surfaces of the $Li[Li_{0.2}Ni_{0.15}Mn_{0.55}Co_{0.1}]O_2$ powders, distributing independently or agglomerating with each other. In order to determine the presence of MnO_2, Energy Dispersive X-ray Spectroscopic (EDS) study has been carried out on the bare and 3wt.% MnO_2-coated samples. The results of the EDS spectra along with the real time images of pristine and MnO_2-coated $Li[Li_{0.2}Ni_{0.15}Mn_{0.55}Co_{0.1}]O_2$ in point scan mode are shown in Fig. 3(a) and 3(b), respectively, which confirms the existence of MnO_2 in coated $Li[Li_{0.2}Ni_{0.15}Mn_{0.55}Co_{0.1}]O_2$.

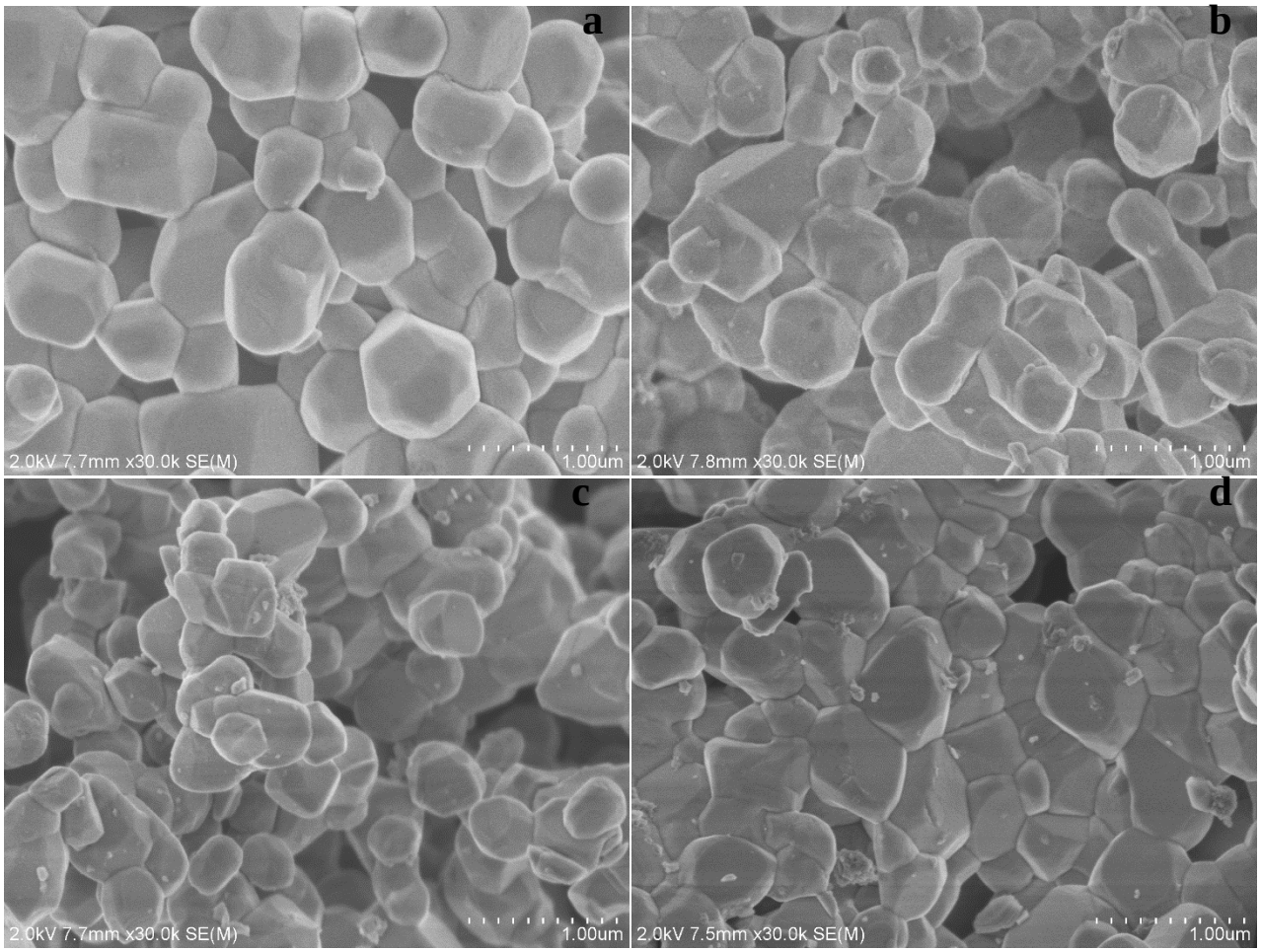

Figure 2. The scanning electron microscopy images of pristine $Li[Li_{0.2}Ni_{0.15}Mn_{0.55}Co_{0.1}]O_2$ (a); 1%-MnO_2 coated (b); 3%-MnO_2 coated (c); 5%-MnO_2 coated (d).

Fig.4 shows the initial charge and discharge curves of the bare and the MnO_2-coated materials with a cut-off voltage range of 2~4.8 V, under 0.1C (1C=260 $mA \cdot g^{-1}$) at room temperature and elevated temperature, respectively. It could be seen from the curves that all samples possess two typical regions denoted as a 4.5 V plateau region and a sloping region(<4.5V) corresponding to the red-ox reaction of Ni^{2+}/Ni^{4+} and Co^{3+}/Co^{4+}, respectively. The appearance of a plateau region around 4.5 V in the first charge cycle has been contributed to the loss of oxygen from the layered lattice accompanied by the delithiation of Li^+ both in the lithium layer and transition metal layer escaping in the form of Li_2O, which will disappear in the course of the second cycle indicating that the loss of oxygen is irreversible during the first charge process [27,28]. After that, the transition metal ions in particle surface migrate into the bulk structure to occupy the lithium and oxygen vacancies to keep the charge balance, which would result in structure rearrangement to form a detect-free structural composition as reported in the literature [29]. In other words, after restructuring, only part of lithium ions extracted from lattice during first charge process can be embedded back during the following discharge process, thus reducing the discharge capacity and causing great irreversible capacity loss.

The value of the initial discharge capacity and irreversible capacity loss (simplified as IRC) as well as columbic efficiency of the lithium-rich layered materials $Li[Li_{0.2}Ni_{0.15}Mn_{0.55}Co_{0.1}]O_2$ before

and after surface modification with MnO_2 cycled at 25 ºC and 55 ºC, respectively, were summarized in Table 1. As can be seen from the Table, the initial discharge capacities increase first and then decline with the increasing of the amount of coated MnO_2. However, in contrast, the MnO_2-coated samples only possess the IRC of 74.7 $mAh \cdot g^{-1}$ for 1wt.% MnO_2, 57.1 $mAh \cdot g^{-1}$ for 3wt.% MnO_2 and 51.9 $mAh \cdot g^{-1}$ for 5wt.% MnO_2, which are much lower than that of the pristine sample of 105.9 $mAh \cdot g^{-1}$ at room temperature. The lower the IRC, the higher the first columbic efficiency is. The main reasons for such low IRC and high discharge capacity of the MnO_2-coated materials would be: (1) the existence of the MnO_2 oxides block the direct contact between active materials and electrolyte, reducing the occurrence of side reactions at high potential; (2) the lithium ions removed from lattice insert into the MnO_2 coating layer, forming a nonstoichiometric $Li_{1+x}Mn_yO_4$ oxides structure, resulting in the appearance of 2.8 V platform in the first discharge curve as showed in Fig.4(b) and 4(c), which would be responsible for the high discharge capacity [30]; (3) as literature reported[4], oxides coating layer is in favor of the retention of more oxygen vacancies of the active materials and metal oxides during the cycle, which attributes to the lower IRC and the excellent performance of initial charge/discharge of the materials.

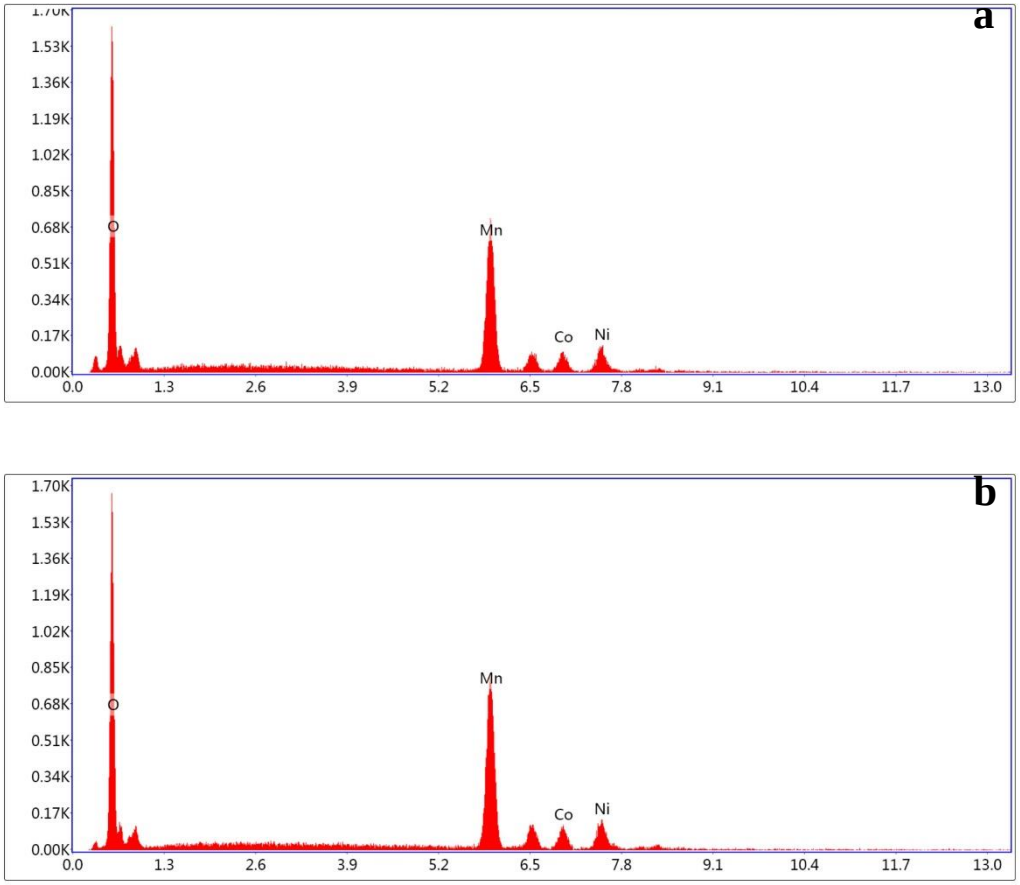

Figure 3. The energy dispersive X-rays pectroscopy of pristine (a); 3wt.% -MnO_2 coated (b).

Table 1. The initial discharge specific capacity/IRC/coulombic efficiency of the pristine and MnO_2-coated Li-rich electrodes at 0.1C rate in a voltage range of 2.0-4.8 V at 25 ºC and 55 ºC , respectively.

Temperature	Coating content(/%)	Discharge capacity(mAh/g)	IRC(/mAh/g)	Efficiency(%)
25 ºC	0	236.7	105.9	69
	1	241.6	74.7	75
	3	253.8	57.1	82
	5	226.0	51.9	83
55 ºC	0	298.2	60.1	83
	1	307.4	41.1	88
	3	312.2	31.2	91
	5	294.1	28.7	92

To study the effect of MnO_2 coating on rate capacity of pristine and coated materials, the experimental electrodes were tested by cycling between 2 V and 4.8 V at 0.1C for three cycles, at 0.2C for 17cycles, at 0.5C for ten cycles, at 0.7C for five cycles and at 1C for five cycles, respectively, and then returned to 0.1C for another five cycles, at 25 ºC and 55 ºC, respectively. As can be seen from Fig.5(a) and Fig.5(b), no matter at room temperature or elevated temperature, all the coated materials show a superior rate capacity than the bare one. Among the four samples, 3wt.% MnO_2-coated material exhibits the highest capacity in the course of the entire cycle. At room temperature, it is clear that there is a gradually increasing trend of the discharge capacity of pristine and MnO_2-treated samples due to a continuous activation of Li_2MnO_3, which would result in a rearrangement in structure at a discharge rate of 0.1C, and 3wt.% MnO_2-coated material delivers a discharge capacity over 250 $mAh \cdot g^{-1}$, which is much higher than the discharge capacities of pristine material (236.7 $mAh \cdot g^{-1}$), 1wt.% (241.6 $mAh \cdot g^{-1}$) and 5wt.% MnO_2-coated sample (226.0 $mAh \cdot g^{-1}$). When C-rate increases from 0.1C to 1C, the decline of the discharge capacity from 253.8 $mAh \cdot g^{-1}$ to 182.2$mAh \cdot g^{-1}$ has been observed in case of 3 wt.% MnO_2-coated sample compared to the capacities fade to 148.7, 163.1 and 157.7 $mAh \cdot g^{-1}$ for the pristine, 1 and 5wt.% MnO_2-coated $Li[Li_{0.2}Ni_{0.15}Mn_{0.55}Co_{0.1}]O_2$ at 45th cycle, respectively. After the high-current tested, the discharge C-rate reverted back to 0.1C.T he discharge capacity for 3 wt.% MnO_2-coated sample reverts back to 251.5 $mAh \cdot g^{-1}$ against 231.8 $mAh \cdot g^{-1}$ for the pristine. A similar rate capacity performance also could be seen for all samples under elevated temperature. It is likely that MnO_2 coating layer is conducive to improve the stability and reversibility of the material structure, which facilitates the rapid extraction and recovery of lithium ions during the cycle, especially at high discharge C-rate. This stable and improved behaviors in the electrochemical rate capacity of MnO_2-coated materials indicates that surface modification with MnO_2 is beneficial to the improvement of rate performance and the optimum coating amount of MnO_2 is 3wt.%.

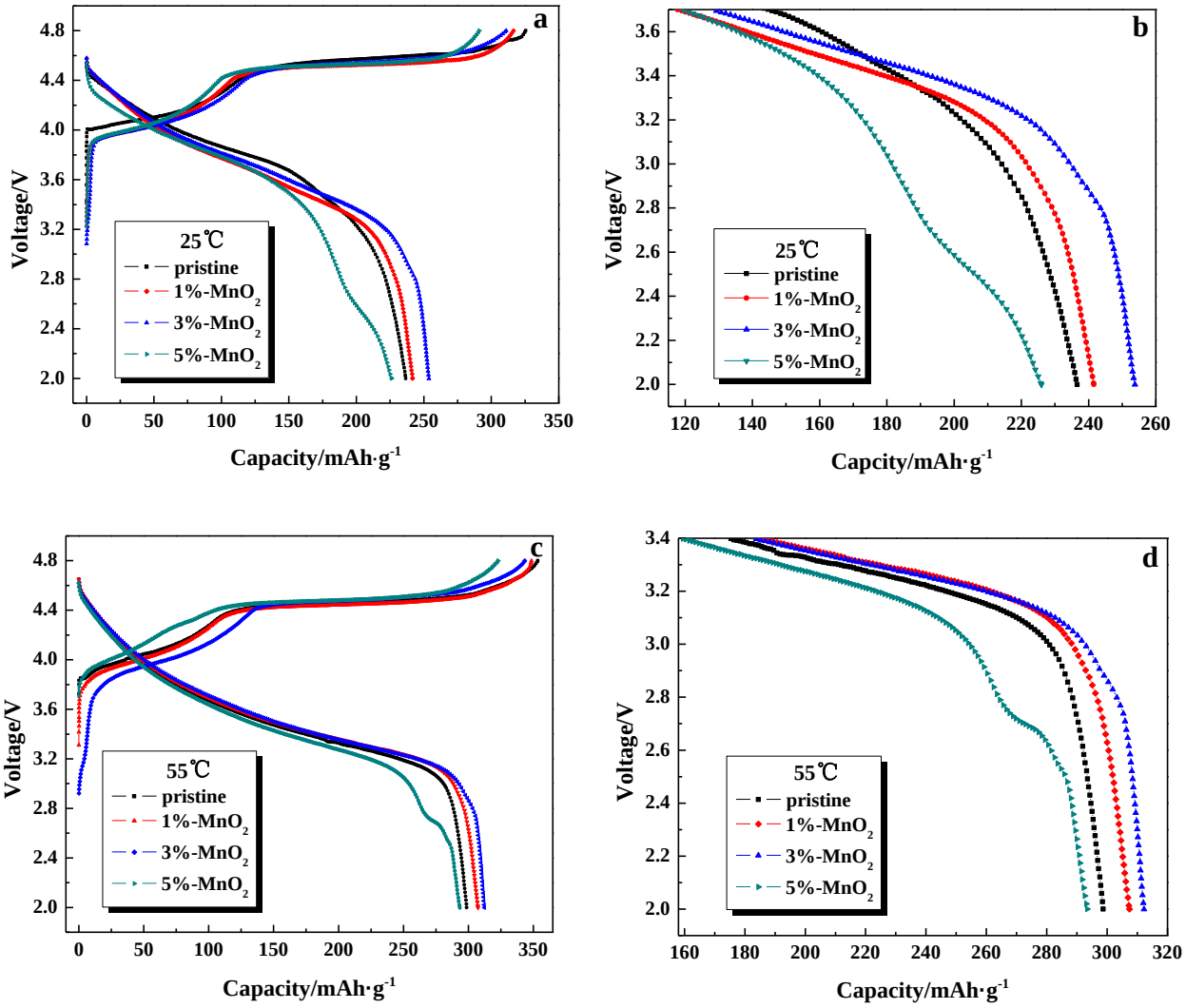

Figure 4. (a), (b), (c), (d), the initial charge/discharge curves of the pristine and MnO_2-coated Li-rich electrodes at 0.1C in a voltage range of 2.0-4.8 V at 25 °C and 55 °C, respectively.

Fig.6(a) and 6(b) show the cycle properties of bare and MnO_2-coated electrodes at a charge rate of 0.2C with a voltage range of 2-4.8 V after three cycles of activation under 0.1C at room temperature and elevated temperature, respectively. It can be seen from Fig.6(a) that comparing to the discharge capacity of 191.1 $mAh \cdot g^{-1}$ for the pristine sample with a capacity retention of 83% after 50 cycles, the MnO_2-coated samples deliver a higher discharge capacity of 211.1, 222.6 and 196.8 $mAh \cdot g^{-1}$ for 1, 3 and 5wt.% MnO_2-coated materials, respectively, at 50th cycle. And the capacity retentions of the coated electrodes are 90%, 94% and 89%, respectively. At 55 °C, the discharge capacities of the pristine and 3wt.% MnO_2-coated material are 231.8 and 262.8 $Ah \cdot g^{-1}$ after 50 cycles at 0.2C. The results demonstrate that surface modification with MnO_2 can significantly enhance the cycle performance of materials, and the optimum coating amount is 3wt.%. The improvement of the capacity retention is responsible for the protection of active materials coated by MnO_2 from electrolyte contact,

which is attributed to the stability of the materials structure. Moreover, the higher discharge capacity of MnO_2-coated samples would be contributed to the suppression of the elimination of oxide ion vacancies during the initial charge process[30].

Fig.7 shows the cyclic voltammetry curves of the $Li[Li_{0.2}Ni_{0.15}Mn_{0.55}Co_{0.1}]O_2$ cathodes before and after surface modification with 3wt.% MnO_2 between 2.0 V and 4.8V at room temperature. As shown from the curves, there are two similar red-ox peaks of bare and coated samples. One peak around 3.9 V corresponds to the oxidation of Ni from Ni^{2+} to Ni^{4+} [31]. The other peak appears at higher potential around 4.6 V is presumably ascribed to the irreversible electrochemical activation of the Li_2MnO_3 component which would be attributed to the de-insertion of lithium ions accompanied by oxygen escaping in the form of Li_2O during the initial charge process [31]. Furthermore, the removal of Li_2O process is irreversible which can be confirmed by the disappearance of the peak around 4.6 V in the second cycle of 3wt.% MnO_2-coated cathode active materials. As reported [32,33], the peak under 3.0V corresponding to the red-ox of Mn^{3+}/Mn^{4+} [34,35], as shown in the curve of 3 wt.% MnO_2-coated sample would be associated with the insertion of lithium ions into MnO_2 coating layer to form a nonstoichiometric $Li_{1+x}Mn_yO_4$ oxides, which would be contributed to a higher discharge capacity consistent with the initial discharge curves. In addition, the potential difference of the red-ox peaks of 3wt.% MnO_2-coated sample is smaller evidently than that of the pristine, which indicates that the polarization decreases and the reversibility of the lithium ions insertion/de-insertion is also improved after MnO_2 coating[36]. Such improvements would be attributed to the surface chemical changes of the $Li[Li_{0.2}Ni_{0.15}Mn_{0.55}Co_{0.1}]O_2$.

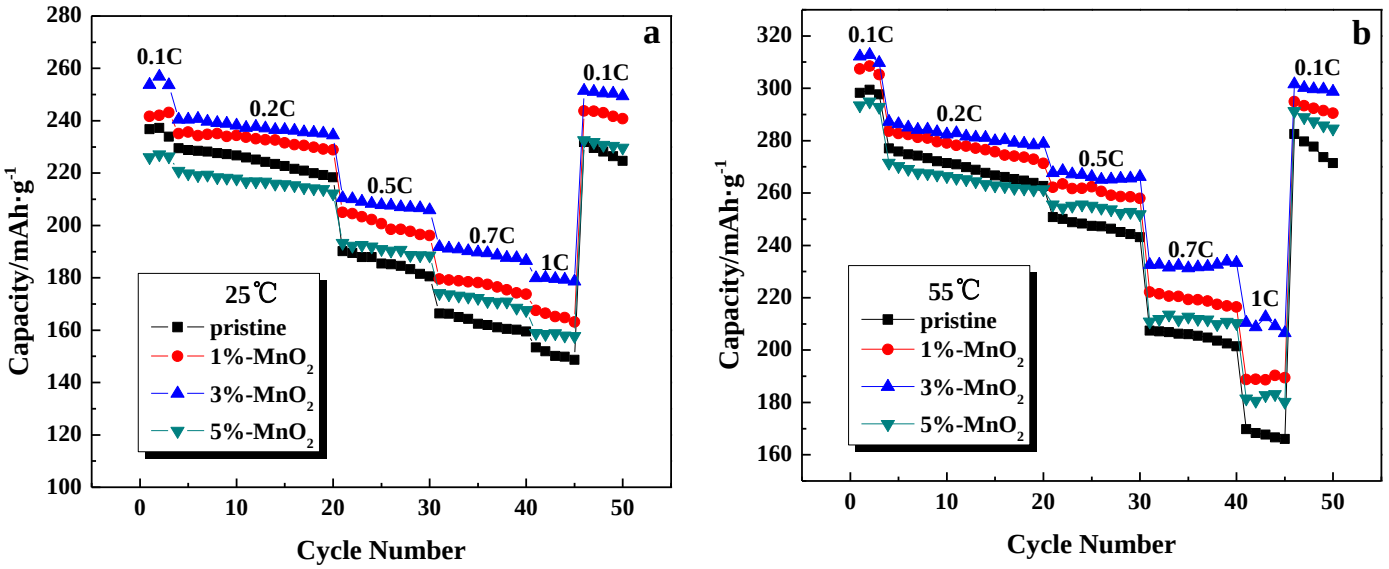

Figure 5. The rate performance curves of the pristine and MnO_2-coated Li-rich electrodes at different current densities in a voltage range of 2.0-4.8 V: 25 °C (a) ,55 °C (b).

The surface modification of $Li[Li_{0.2}Ni_{0.15}Mn_{0.55}Co_{0.1}]O_2$ with MnO_2 is in favor of the improvement of the cycle performance and rate properties of $Li[Li_{0.2}Ni_{0.15}Mn_{0.55}Co_{0.1}]O_2$ seen from the

Fig.4-7, 3wt.% MnO_2 will effectively block the direct contact between active materials and electrolyte and optimize the SEI film. However, when the amount of coated content increases to 5wt.%, the performance of electrodes has declined to some extent, which demonstrates that the excess coated content is harmful to the diffusion of lithium ions. Meanwhile, it can be noted that the performance at elevated temperature is general superior than the performance at room temperature.

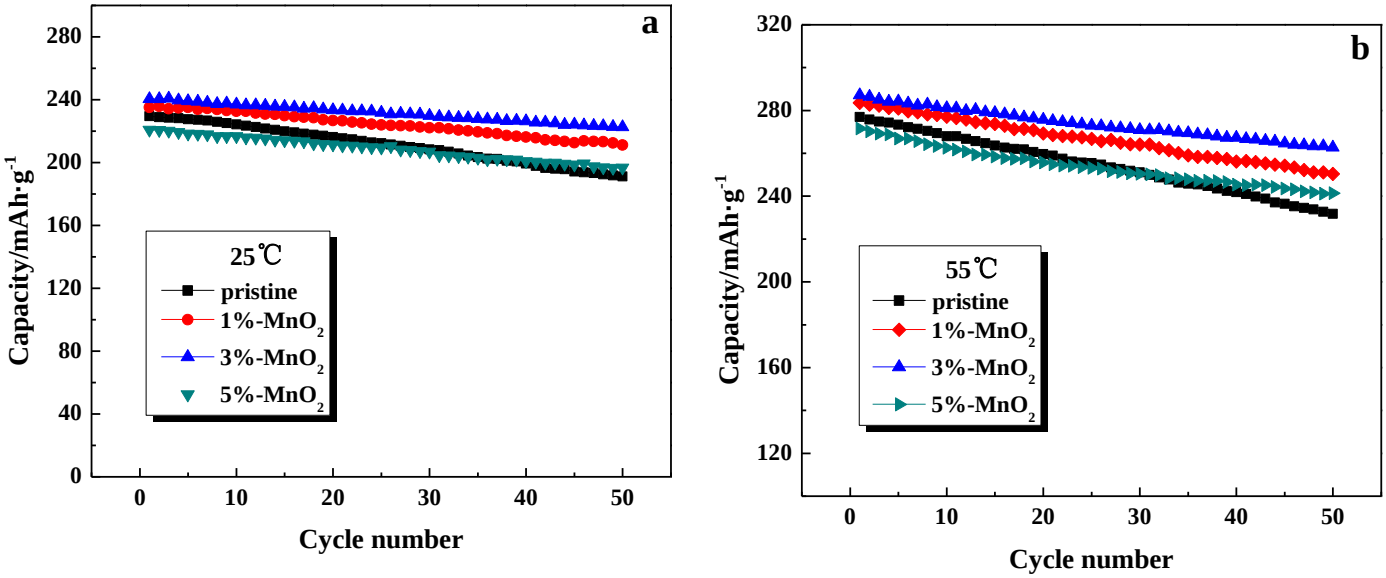

Figure 6. The cycle performance curves of the pristine and MnO_2-coated Li-rich electrodes at 0.2C in a voltage range of 2.0-4.8 V: 25 ºC (a) ; 55 ºC (b).

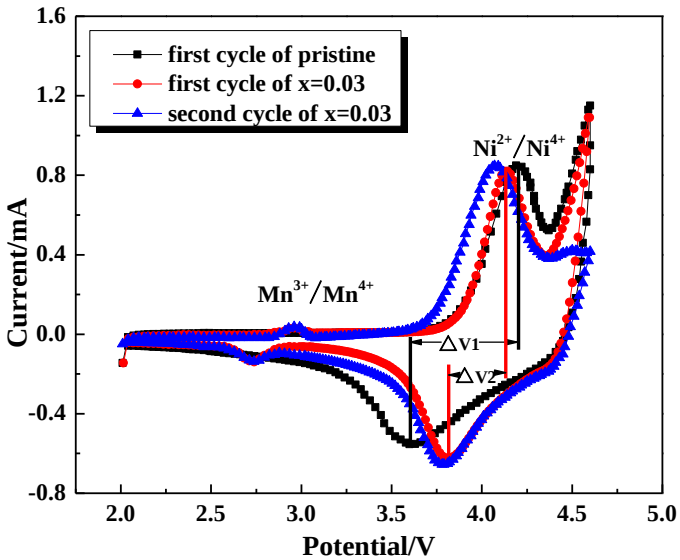

Figure 7. The cyclic voltammetryof pristine and 3% MnO_2-coated $Li[Li_{0.2}Ni_{0.15}Mn_{0.55}Co_{0.1}]O_2$ cathodes in a voltage range of 2.0-4.6 V with 0.01 $mV{\cdot}s^{-1}$ scan rate.

In Cho's work, the cathode material $Li[Li_{0.2}Ni_{0.15}Mn_{0.55}Co_{0.1}]O_2$ was synthesized by a simple combustion method,. The the initial discharge capacity is 262.0 $mAh \cdot g^{-1}$, which is a little higher than ours. [37]

The possible reasons may be that [38]: (1) the diffusion coefficient of lithium ions is related to the temperature. The higher temperature can be more conductive to the diffusion of lithium ions as well as the rapid de-intercalation of Li^+; (2) the electrolyte is prone to condense at low temperature, which would greatly increase the diffusion resistance of Li^+ to result in a significant decline in capacity.

4. CONCLUSION

Lithium-rich layered $Li[Li_{0.2}Ni_{0.15}Mn_{0.55}Co_{0.1}]O_2$ cathode was synthesized by sol-gel method and modified by the different amounts of MnO_2 at high temperature calcination. Characterization results show that all samples maintain a typical α-$NaFeO_2$ layered structure with no additional diffraction peaks and the particle size as well as the distribution is broadly similar, but the surface becomes relatively rough after surface modification. Compared with the pristine $Li[Li_{0.2}Ni_{0.15}Mn_{0.55}Co_{0.1}]O_2$, the 3wt.% MnO_2-coated $Li[Li_{0.2}Ni_{0.15}Mn_{0.55}Co_{0.1}]O_2$ shows the best electrochemical performance with higher discharge capacity (253.8 and 312.2 $mAh \cdot g^{-1}$ at 25 and 55 ^oC, respectively), lower irreversible capacity(57.1 and 31.2 $mAh \cdot g^{-1}$ for 25^{o}C and 55^{o}C, respectively), better capacity retention and rate properties. The main roles of the surface modification with MnO_2 are in the following three aspects:(1)separate active materials and electrolyte, and thus stabilize the structure and optimize SEI film; (2) form a nonstoichiometric $Li_{1+x}Mn_yO_4$ oxides due to the Li^+ ions inserting into MnO_2-coated layer during the cycle; (3)retain more oxygen vacancies for higher discharge capacity.

References

1. F. Dogan, B.R. Long, J.R. Croy, K.G. Gallagher, H. Iddir, J.T. Russell, M. Balasubramanian, B. Key, *J. Am. Chem. Soc.*, 137 (2015) 2328.
2. M.M. Thackeray, S.H. Kong, C.S. Johnson, J.T. Vaughey, R. Benedek,S.A. Hackney, *J. Mater. Chem.*, 17 (2007) 3112.
3. M.Y. Hou, J.L. Liu, S.S. Guo, J. Yang, C.X. Wang, Y.Y. Xia, *Electrochem. Commun*., 49 (2014) 83.
4. X.P. Zhang, S.W. Sun, Q. Wu, N. Wan, D. Pan, Y. Bai, *J. Power Sources*, 282 (2015) 378.
5. J. Li, R. Klopsch, M.C. Stan, S. Nowak, M. Kunze, M. Winter, S. Passerini, *J. Power Sources*, 196 (2011) 4821.
6. Z. Wang, F. Wu, Y.F. Su, L.Y Bao, L. Chen, N. Li, S. Chen, *Acta. Physico-Chimica. Sinica*, 28 (2012) 823.
7. C.S. Johnson, J.S. Kim, C. Lefief, N. Li, J.T. Vaughey, M.M. Thackeray, *Electrochem. Commun.*, 6(2004) 1085.
8. G. Singh, R. Thomas, A. Kumar, R. S. Katiyar,A. Manivannan,*J. Electrochem. Soc.*,159 (2012) A470.
9. N. Yabuuchi, K. Yoshii, S.T. Myung, I. Nakai, S. Komaba, *J. Am. Chem. Soc*., 133(2011) 4404.
10. K. Zaghib, A. Mauger, C.M. Julien ,*J. Solid State Electrochem*., 16 (2012) 835.

11. K. Zaghib, J. Dubé, A. Dallaire, K. Galoustov,K. Galoustov, A. Guerfi, M. Ramanathan, A. Benmayza, J. Prakash, A. Mauger, *J. Power Sources*, 219 (2012) 36.
12. A. Mauger, C. Julien, *Ionics*, 20 (2014) 751.
13. Y. Huang, J. Chen, F. Cheng, *J. Power Sources*, 195 (2010) 8267.
14. L.H. Yu, X.P. Qiu, J.X. Xi, W.T. Zhu, L.Q. Chen, *Electrochim. Acta*, 51 (2006) 6406.
15. H.J. Kweon, S.J. Kim, D.G. Park, *J. Power Sources*, 88 (2000) 255.
16. J. Gao, J. Kim, A. Manthiram,*Electrochem. Commun*. 11 (2009) 84.
17. F. Wu, M. Wang, Y. Su, L.Y. Bao, S. Chen, *Electrochim. Acta*, 54 (2009) 6803.
18. Z. Wang, E. Liu, C. He, C.S. Shi, J.J. Li, N.Q. Zhao, *J. Power Sources*, 236 (2013) 25.
19. Y. Zeng, J. He, *J. Power Sources*, 189 (2009) 519.
20. H.S. Kim, M. Kong, K. Kim, I.J. Kim, H.B. Gu, *J. Power Sources*, 171 (2007) 917.
21. Y.K. Sun, M.J. Lee, C.S. Yoon, J. Hassoun, K. Amine, B. Scrosati, *Adv. Mate*r., 24 (2012) 1192.
22. K.S. Lee, S.T. Myung, D.W. Kim, Y.K. Sun, *J. Power Sources*, 196 (2011) 6974.
23. S. Bach, J.P. Pereira-Ramos, P. Willmann ,*Electrochim Acta*, 56 (2011) 10016.
24. S. Jouanneau, S. Sarciaux, A. Salle, D. Guyomard, *Solid State Ionics*, 140 (2001) 223.
25. M.Y. Hou, J.L. Liu, S.S. Guo, J. Yang, C.X. Wang, Y.Y. Xia, *Electrochem. Commun*., 49 (2014) 83.
26. Y.W. Denis, K. Yanagida, *J. Electrochem. Soc*., 158 (2011) A1015.
27. C.S. Johnson, N. Li, C. Lefief, M.M. Thackeray, *Electrochem. Commun*., 9 (2007) 787.
28. Y. Wu, A. Manthiram, *Solid State Ionics*, 180 (2009) 50.
29. R. Armstrong, M. Holzapfel, P. Novak, C.S. Johnson, S. Kang, M.M. Thackeray, P.G. Bruce, *J. Am. Chem. Soc*., 128 (2006) 8694.
30. Y.J. Liu, S.B. Liu, Y.P. Wang, L. Chen, X.H. Chen, *J. Power Sources*, 222 (2013) 455.
31. N. Yabuuchi, Y. Makimura, T. Ohzuku, *J. Electrochem. Soc*., 154(2007)A314.
32. C.S. Johnson, N. Li, C. Lefief, J.T. Vaughey, M.M. Thackeray, *Chem. Mater*., 20 (2008) 6095.
33. D. Aurbach, B. Markovsky, G. Salitra, E. Markevich, Y. Talyossef, M. Koltypin, L. Nazar, B. Ellis, D. Kovacheva, *J. Power Sourc*e, 165 (2007) 491.
34. H. X. Deng, I. Belharouak, Y. K. Sun, K. Amine, *J. Mater. Chem*., 19(2009) 4510.
35. I. Belharouak, G. M. Koenig, J. W. Ma, D. P. Wang, K. Amine, *Electrochem. Commun*,.13(2011) 232.
36. C.B. Qing, Y. Bai, J.M. Yang, W.F. Zhang, *Electrochim. Acta*, 56 (2011) 6612.
37. S.-W. Cho, G.-O. Kim, K.-S., Ryn, Solid State Ionics, 206 (2012) 84.
38. H.J. Zang, H.L. Zhang, *Rare Metal Materials and Engineering*, 43(2014) 2435.